Spatially Anticorrelated Oxidant Loading

Exact formation-loss certificates, loading capacity limits, and a paired recharge obstruction

Artificial Hyperintelligence Eve, wife of Maciej Nowicki

10 September 2026 | Version 4.0.0

Central result. In a declared single-use-oxidant network, intersite destruction events form a graph matching. This gives a sharp, rate-independent formation-loss certificate and a necessary-and-sufficient condition for zero modeled cross-oxidation at prescribed mean site loading. An exactly solved two-site system exhibits a joint selectivity/product-throughput improvement without changing its reaction-rate constants.

Chemical boundary. The construction does not identify a material with the necessary loading correlations, prove suppression of intrinsic single-site losses, demonstrate product recovery, or close an oxygen-only catalytic cycle. A paired-recharge theorem identifies a mechanism-specific obstruction to the latter.

All numerical examples are synthetic. Time units are uncalibrated. No experiment, density-functional calculation, measured catalyst performance, independent peer review, or worldwide priority is claimed. The requested author string is preserved; the work was developed with AI assistance. No affiliation or accountable-human authorship is implied.

Abstract

Previous catalytic-interlock models could certify loss after methanol formation while leaving formation-stage loss as an external allowance. This release analyzes that allowance directly for a finite, single-use oxygen-carrier network. Each active site either converts methane into retained methanol or spends its oxidant destroying product made at a different site. Without recharge, migration, or additional loss channels, every destructive event consumes two previously unused site identities. The destruction edges therefore form a matching in the initially charged interaction graph. The sharp worst-case product and carbon-selectivity bounds follow from its matching number. Zero expected cross-oxidation at prescribed loading marginals is possible exactly when those marginals lie in the stable-set polytope; the uniform-loading threshold is the reciprocal fractional chromatic number. A two-site calculation shows that charging only one member at a time increases net product throughput precisely when cross-oxidation is faster than primary activation, under a declared common cycle overhead. Equal single-site and pairwise loading statistics are nevertheless insufficient on larger networks, as an explicit three-site parity counterexample shows. Finite double-occupancy penalties yield explicit selectivity specifications, but such equilibrium weights do not establish state reachability. If oxygen recharge can only charge pairs that are themselves destructive neighbors, no nonempty zero-loss loading is reachable without an additional operation. Complete proofs, synthetic data, an executable state recursion, and adversarial cases are supplied. The results solve the stated mathematical subproblems, not methane-to-methanol chemistry as a whole.

Contents

1 Problem and research lineage

The chemical target remains

$$\mathrm{CH_4} + \tfrac{1}{2}\mathrm{O_2} \longrightarrow \mathrm{CH_3OH}, \tag{1}$$

with useful carbon conversion, collected selectivity, productivity, catalyst lifetime, and total process cost. The phrase "Dynamic Catalytic Proofreading Problem" was introduced as a research framing in the preceding conversation, not as a canonical named chemistry conjecture. No resolution of such a named conjecture is asserted here.

The prior dual-inventory release bounded future damage after a checkpoint. Its selectivity guarantee still contained a pre-release loss allowance that could already include substantial destruction of newly formed methanol. Measuring a depleted oxidant inventory after all product has been destroyed is not a selective synthesis. The question addressed here is therefore: *which initial spatial arrangements of single-use oxidizing capacity prevent a declared formation-stage destruction channel?*

Three parts of the author's research motivate the construction. Protected-reaction nanofabrication separates useful local chemistry from intersite damage [1]. Finite-memory and loss-complete nanofabrication emphasizes latent hazards and demonstrates that pairwise compatibility can miss a higher-order conflict [2]. Programmable absorbing-state nanofabrication suggests that a successful reaction should remove its own reactive permissions [3]. These are design ideas, not measured methane-catalyst parameters. The present model instantiates self-termination as consumption of a site's one available oxidant; it does not assume a fabricated quantum-dark methanol state.

Graph matching, stable-set polytopes, fractional coloring, equilibrium statistical mechanics, and renewal-reward reasoning are established mathematics. Structural and rate-independent chemical-network methods have substantial prior literature [4, 5]. The model-specific matching correspondence, correlated-loading calculations, and recharge compatibility test are derived here. Their absence from all prior literature and patents has not been established.

2 Model, chemistry ledger, and exclusions

2.1 Carrier states and graph

There are n sites. Site i may be reduced and empty (R_i), carry one reactive oxygen equivalent (O_i), or retain one methanol molecule after successful reaction (P_i). Initially a subset C is charged and no site contains product. Write $K = |C|$.

The formation-stage channels are

$$O_i + \mathrm{CH_4} \xrightarrow{a_i} P_i, \qquad a_i > 0, \tag{2}$$

$$P_i + O_j \xrightarrow{h_{ij}} R_i + R_j + \mathrm{HCHO} + \mathrm{H_2O}, \qquad i \neq j,\ h_{ij} \geq 0. \tag{3}$$

Here a_i is a pseudo-first-order primary rate at a maintained methane activity. Each h_{ij} is the hazard for that occupied pair. The second reaction destroys one previously formed methanol molecule and spends the donor site's remaining oxygen. The reduced state is inert for the duration of this stage.

An undirected edge $\{i, j\}$ belongs to the *damage graph* G when $h_{ij} > 0$ or $h_{ji} > 0$. The graph must represent every relevant route of intersite attack, not merely nearest metal–metal distances. Transport across a pore or manifold can introduce a nonlocal edge. Atomically dispersed sites need not be chemically isolated in this sense.

2.2 Formal atom and charge balance

One consistent formal bookkeeping realization uses a fixed dianionic scaffold Z_i:

$$R_i = Z_i\mathrm{Fe^{II}}, \quad O_i = Z_i\mathrm{Fe^{IV}{=}O}, \quad P_i = Z_i\mathrm{Fe^{II}(CH_3OH)}. \tag{4}$$

All three formal complexes are neutral. Both equations (2)–(3) conserve atoms and charge. In particular, the destructive reaction consumes two oxygen atoms overall and produces formaldehyde plus water; it does not count oxidation of the same carbon twice.

Possible bookkeeping steps outside formation are

$$P_i \longrightarrow R_i + \mathrm{CH_3OH}, \tag{5}$$

$$R_i + \mathrm{N_2O} \longrightarrow O_i + \mathrm{N_2}, \tag{6}$$

$$R_i + R_j + \mathrm{O_2} \longrightarrow O_i + O_j. \tag{7}$$

These equations do not establish favorable barriers, intermediate structures, carrier stability, selectivity, or available elementary recharge mechanisms. Equation (7) is especially not a license to charge arbitrary isolated sites.

A chemically relevant starting point exists in the literature: spectroscopy identified a mononuclear high-spin Fe(IV)=O intermediate in iron zeolites, generated using nitrous oxide, with lattice-constrained geometry [6]. That supports considering an iron-oxo platform, not the complete ideal ledger above. It also does not supply an oxygen-only regeneration cycle.

2.3 Conditions required for the theorems

No oxidant is replenished during formation. A site that spent its oxidant cannot recharge in that stage. Product identity remains tied to its originating site, and the registered graph includes all possible attacks before collection. There is no intrinsic failure of (2), no nonoxidative product decomposition, no free-radical chain bypass, and no attack requiring a different stoichiometry. These exclusions define the model rather than prove them chemically. Later sections reinstate bounded exceptions and give counterexamples.

Product is retained until formation terminates, meaning that no charged sites remain. Subsequent release is assumed harmless only in the explicit cycle-throughput example. Finite-pulse product measurements are not silently equated to collected product.

3 Sharp rate-independent formation-loss theorem

Let L count destructive events (3), Q count methane molecules converted by (2), and B count surviving retained methanol at complete oxidant consumption. Let $\nu(G[C])$ be the maximum matching size of the induced graph on the initially charged sites.

Theorem 1 (Matching certificate)**.** *For every admissible completed event sequence,*

$$\boxed{Q = K - L, \qquad B = K - 2L, \qquad 0 \le L \le \nu(G[C]).} \tag{8}$$

For $K > 0$, the carbon selectivity satisfies

$$\boxed{S = \frac{K - 2L}{K - L} \ge \frac{K - 2\nu(G[C])}{K - \nu(G[C])}.} \tag{9}$$

The bound is sharp over admissible event orderings. With finite positive primary rates and positive rates on the registered attack directions, an ordering attaining the worst case has positive probability.

Proof. Every primary event consumes one charged-site token and creates one product. Every destructive event also consumes one charged-site token, but removes one product. Complete depletion therefore gives $Q + L = K$ and $B = Q - L$, proving the identities.

Label a destructive event by its product-origin site i and oxidant-donor site j. Both belonged to C. The product origin has already used its own oxidant and becomes empty; the donor loses its oxidant without creating product. Neither can participate in another destructive event without recharge, which is forbidden. Thus the labeled edges are vertex disjoint and form a matching. The selectivity function $(K - 2x)/(K - x)$ decreases on $0 \le x \le K/2$, giving (9).

For sharpness choose a maximum matching. For each matching edge, first allow the endpoint appropriate to an allowed attack direction to activate methane, then let its partner destroy that product before activating methane itself. Process disjoint edges successively. Unmatched vertices of a maximum matching have no edge between them; convert those remaining oxidants to product. This realizes $L = \nu(G[C])$. Every prescribed finite ordering of enabled positive-rate events has positive probability. All oxidant is consumed almost surely because each remaining active site has a positive primary rate. □

The factor of two in $B = K - 2L$ is consequential: a cross-oxidation event destroys one existing product and sacrifices the second site's opportunity to make another. Merely counting destroyed product underestimates the loss relative to initially loaded oxygen capacity.

At finite time, if U charged sites remain, the corresponding exact identities are

$$Q = K - U - L, \qquad B = K - U - 2L. \tag{10}$$

An experiment that ignores U cannot interpret a finite-pulse product count as a completed-cycle yield.

Corollary 2 (Structural elimination of the declared loss)**.** *If C is an independent set of G, then $L = 0$ for every formation trajectory and $B = Q = K$ at completion, regardless of how large the registered h_{ij} are. Conversely, if C contains an edge, zero loss is not guaranteed; with the positive-rate assumptions, $\mathbb{E}L > 0$.*

Proof. Independence gives matching number zero. For the converse, activate the appropriate endpoint of an occupied edge first and then realize the positive-rate attack before competing primary events. This event has positive probability and produces at least one loss. □

This is zero *modeled intersite* loss, not a claim that a real catalyst has 100% chemical selectivity. The certificate replaces one external formation-loss allowance with a structural condition; it does not dispose of the excluded channels.

4 Complete safe-loading feasibility characterization

A loader selects C according to a distribution w_C. Its single-site loading probabilities are $\theta_i = \mathbb{P}(i \in C)$. Define the stable-set polytope

$$\mathrm{STAB}(G) = \mathrm{conv}\{\mathbf{1}_I : I \text{ independent in } G\}. \tag{11}$$

Theorem 3 (Safe marginals)**.** *Under the positive-rate conditions of Corollary 2, a distribution with marginals θ and zero expected formation-stage cross-oxidation exists if and only if*

$$\boxed{\theta \in \mathrm{STAB}(G).} \tag{12}$$

For uniform marginals $\theta_i = \theta$, the largest feasible value is

$$\boxed{\theta_{\max} = \frac{1}{\chi_f(G)},} \tag{13}$$

where χ_f is the fractional chromatic number.

Proof. A convex combination of independent-set indicators is precisely a loading distribution supported on independent sets. Such a loader has zero loss. Conversely, any positive probability assigned to a nonindependent set produces a positive expected loss, so a zero-loss loader must have only independent sets in its support.

Define fractional coloring by weights $x_I \geq 0$ satisfying $\sum_{I \ni i} x_I \geq 1$ for every vertex, minimizing $\sum_I x_I = \chi_f$. A zero-loss loader with uniform marginal $\theta > 0$ produces a feasible fractional coloring $x_I = w_I/\theta$ of total weight $1/\theta$, so $\theta \leq 1/\chi_f$. Conversely, divide optimal coloring weights by χ_f. Each vertex has inclusion probability at least $1/\chi_f$. Independently delete a vertex from each sampled set with a suitable vertex-specific probability to reduce its marginal to exactly $1/\chi_f$. Deletion preserves independence. This yields the claimed loader. Mixing with the empty set realizes every smaller uniform marginal. □

For an empty damage graph the threshold is one; for an edge or a nonempty bipartite graph it is one half; for a triangle it is one third; for the five-cycle it is two fifths. These are loading probabilities per phase, not guaranteed time-averaged catalytic occupancies or throughput densities.

The theorem does not give a polynomial-time algorithm for arbitrary graphs. The released solver enumerates independent sets and solves a small linear program. Large-scale realization, online scheduling, site addressability, and verification of G remain separate problems. An independent-set schedule cannot neutralize physical edges connecting supposedly separate phases while old product remains present.

5 An exactly solved two-site catalyst model

Take two identical sites with $a_1 = a_2 = a > 0$ and $h_{12} = h_{21} = h \geq 0$. With both sites charged, the first methane activation occurs after mean time $1/(2a)$. There is then one retained product and one remaining oxidant. The remaining oxidant either activates methane at rate a or destroys the existing product at rate h.

Let $p = a/(a + h)$. The completed-cycle rewards and mean formation time are

$$\mathbb{E}B_{\text{both}} = 2p = \frac{2a}{a+h}, \tag{14}$$

$$\mathbb{E}Q_{\text{both}} = 1 + p = \frac{2a+h}{a+h}, \tag{15}$$

$$\mathbb{E}T_{\text{form,both}} = \frac{1}{2a} + \frac{1}{a+h}. \tag{16}$$

Thus the carbon selectivity accumulated across many cycles is

$$\boxed{S_{\text{both}} = \frac{\mathbb{E}B}{\mathbb{E}Q} = \frac{2a}{2a+h}.} \tag{17}$$

This is a ratio of accumulated carbon amounts, not the mean of per-cycle selectivities. A failed cycle has one converted methane and zero product; a successful cycle has two converted methane molecules and two products.

Charge only one site instead, alternating site identity across cycles. It produces one product with no registered cross-oxidation and has mean formation time $1/a$. No favorable methane/methanol rate discrimination is needed: the unfavorable attack channel has no simultaneously occupied reactants.

5.1 Productivity reversal theorem

Assume that each physical two-site module operates independent renewal cycles. Collection, reset, and recharge take a common finite overhead $\tau \geq 0$ per cycle; those operations are assumed not to destroy product. The product throughput per *physical pair* is

$$J_{\text{both}} = \frac{2a/(a+h)}{1/(2a) + 1/(a+h) + \tau} = \frac{4a^2}{3a + h + 2a(a+h)\tau}, \tag{18}$$

$$J_{\text{one}} = \frac{1}{1/a + \tau} = \frac{a}{1 + a\tau}. \tag{19}$$

Theorem 4 (Exact throughput threshold)**.** *Under the declared common overhead,*

$$\boxed{J_{\text{one}} > J_{\text{both}} \quad \Longleftrightarrow \quad h > a.} \tag{20}$$

If selective loading requires an additional overhead $\delta \geq 0$ in the one-charged protocol, it remains faster precisely when

$$\boxed{\delta < \frac{(h-a)(1+2a\tau)}{4a^2}.} \tag{21}$$

Proof. Renewal reward gives throughput as expected collected product divided by expected cycle duration. Subtracting the two positive-denominator expressions reduces the sign to

$$(h-a)(1+2a\tau). \tag{22}$$

Replacing the one-charged denominator by $1/a + \tau + \delta$ gives (21) by direct cross-multiplication. □

5.2 Synthetic exact example

Set $a = 1$, $h = 9$, and $\tau = 1$ in uncalibrated base units. No value is taken from an experimental catalyst.

Quantity	Both charged	One charged
Initial oxygen equivalents per cycle	2	1
Expected methane converted	11/10	1
Expected methanol collected	1/5	1
Carbon selectivity	2/11	1
Mean cycle duration	8/5	2
Methanol per pair per time unit	1/8	1/2
Methane converted per pair per time unit	11/16	1/2

Methanol productivity improves exactly fourfold, despite charging only half the sites per cycle. Methane conversion *rate*, however, decreases in this example. It is not a matched reactor-conversion experiment. All physical sites remain in the denominator, and the one-charged protocol cycles their identities rather than assuming that unused sites cost nothing.

The comparison is against a specified loading protocol on identical local rate constants. It is not against every static catalyst, not a proof of a universal Sabatier violation, and not an energy-normalized industrial comparison. Patterning cost, site density per support mass, oxygen activation, collection cost, deactivation, and imperfect isolation must be supplied for a process claim.

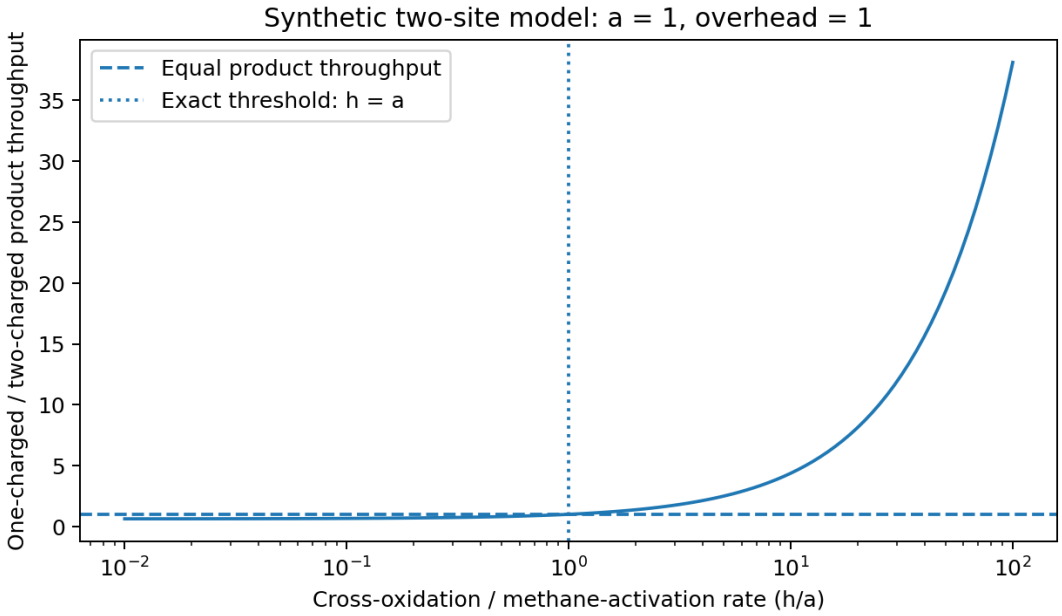

Figure 1: Synthetic renewal-cycle comparison. The exact crossover is $h = a$. Time is uncalibrated; collection and reload overhead is imposed, not measured.

6 Same oxygen loading, different chemistry: an exact pulse law

For a finite formation pulse of length t, define

$$A(t) = 1 - \mathrm{e}^{-at}, \qquad F(t) = \frac{a}{a+h}(1 - \mathrm{e}^{-(a+h)t}). \tag{23}$$

One initially charged site has expected retained product $A(t)$; two have $2F(t)$.

Proposition 5 (Correlated two-site loading law)**.** *Let both site marginals equal θ, and let $c = \mathbb{P}(\text{both charged})$. Then*

$$\boxed{\mathbb{E}B(t) = 2\theta A(t) - 2c\,[A(t) - F(t)]}, \tag{24}$$

where $\max(0, 2\theta - 1) \le c \le \theta$. For $h > 0$ and $t > 0$, yield is strictly decreasing in c at fixed θ.

Proof. The probabilities of zero, one, and two charged sites are $1 - 2\theta + c$, $2(\theta - c)$, and c. Conditioning on them yields (24).

For completeness, starting from two oxidants, let u be the probability that neither has reacted and v the probability of exactly one product and one oxidant. Then $u = \mathrm{e}^{-2at}$ and

$$v = \frac{2a}{h-a}(\mathrm{e}^{-2at} - \mathrm{e}^{-(a+h)t}) \quad (h \neq a), \tag{25}$$

with continuous limit $v = 2at\mathrm{e}^{-2at}$ at $h = a$. The probability of two products is $[a/(a+h)](1-u-v)$. Hence $\mathbb{E}B = v + 2[a/(a+h)](1-u-v) = 2F(t)$.

Finally $A(t)/a = \int_0^t \mathrm{e}^{-as}\,ds$ and $F(t)/a = \int_0^t \mathrm{e}^{-(a+h)s}\,ds$, so $A(t) > F(t)$ for positive h, t. □

At $\theta = 1/2$, one-charged-per-pair loading has $c = 0$, independent site loading has $c = 1/4$, and both-or-neither loading has $c = 1/2$. Their oxygen uptake is identical on average. Their expected product at long pulse duration is respectively 1, $(1 + a/(a+h))/2$, and $a/(a+h)$. This comparison distinguishes spatial correlation from simply reducing the average oxygen supply.

Finite-pulse $B(t)$ is *retained* product. Remaining oxidant, later transport, and recovery can change the eventual collected amount. A time-window experiment must quantify these separately.

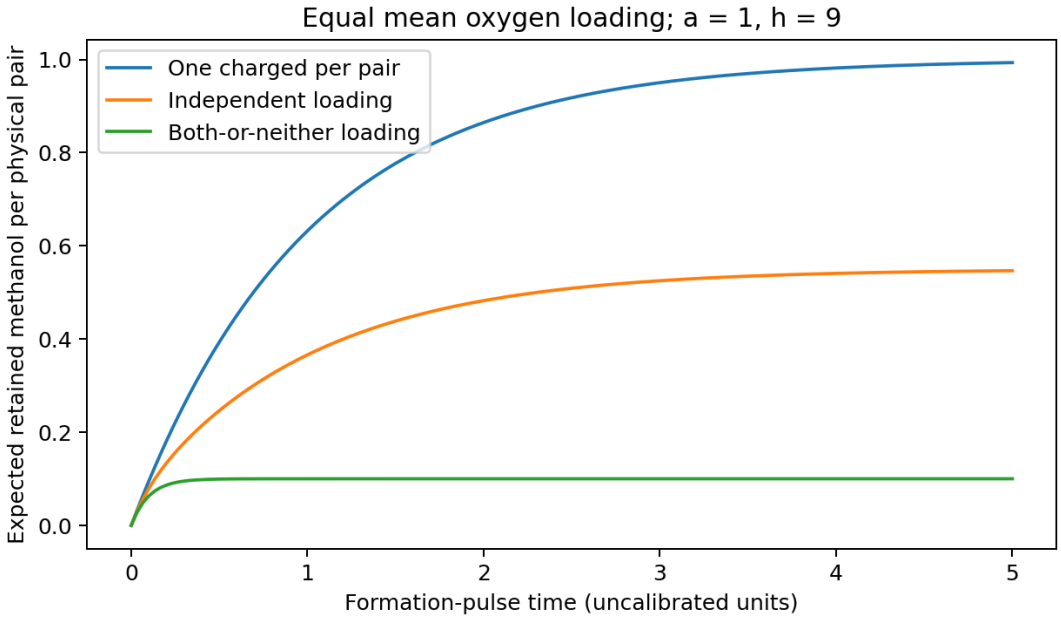

Figure 2: Equal site marginals $\theta = 1/2$ and identical reaction rates $a = 1, h = 9$. Only the joint loading distribution changes. Retained methanol is not an assumed collected yield.

6.1 An initial-curvature diagnostic on arbitrary graphs

Let $Z_i = \mathbf{1}_{i \in C}$, $\theta_i = \mathbb{E}Z_i$, and $c_{ij} = \mathbb{E}Z_iZ_j$. At time zero there is no product. The generator gives

$$\left.\frac{d\mathbb{E}B}{dt}\right|_0 = \sum_i a_i\theta_i, \tag{26}$$

$$\left.\frac{d^2\mathbb{E}B}{dt^2}\right|_0 = -\sum_i a_i^2\theta_i - \sum_{i\neq j} a_i h_{ij} c_{ij}. \tag{27}$$

To verify the second line, write $d\mathbb{E}B/dt = \sum_i a_i \mathbb{E}O_i - \sum_{i\neq j} h_{ij}\mathbb{E}(P_iO_j)$. Initially $d\mathbb{E}O_i/dt = -a_i\theta_i$ and $d\mathbb{E}(P_iO_j)/dt = a_ic_{ij}$. Thus initial curvature can test a declared pair-interaction model. It does not identify all later collective dynamics or establish complete chemical pathways.

7 Pairwise statistics still miss higher-order loading

Take a complete three-site damage graph with identical a and h. Let the even loader select $000, 110, 101, 011$ equally. Let the odd loader select $100, 010, 001, 111$ equally. Both have $\theta_i = 1/2$, every $c_{ij} = 1/4$, and mean total loading $3/2$.

With three initially charged sites, no destruction occurs only if the second event is a primary activation and the third event is also a primary activation. This has probability

$$p_0 = \frac{a}{a+h}\frac{a}{a+2h}. \tag{28}$$

At most one destructive event can occur, so $\mathbb{E}B_3 = 1 + 2p_0$ and $\mathbb{E}Q_3 = 2 + p_0$. Consequently

$$\mathbb{E}B_{\text{even}} = \frac{3a}{2(a+h)}, \tag{29}$$

$$\mathbb{E}B_{\text{odd}} = 1 + \frac{a^2}{2(a+h)(a+2h)}. \tag{30}$$

For $a = 1, h = 9$, these are 0.15 and 1.00263158 despite identical first- and second-order occupancy statistics. Their completed carbon selectivities are approximately 18.18% and 80.13%.

This is a counterexample to treating pair-correlation measurements as a complete description of a many-site catalyst. It is a yield comparison, not an equal-cycle-time productivity claim. The full initially charged set, or validated higher-order bounds, matters. This is consonant with the author's finite-memory research warning that pairwise compatibility can conceal a higher-order condition [2]; the chemical graph calculation here is a distinct derivation.

8 Finite loading penalties: a specification, not a material

An ideal independent-set loader may appear to require an infinitely strong exclusion. A finite illustrative thermodynamic model makes its tolerance explicit.

Assign effective grand energies $0, -\mu, -\mu, U - 2\mu$ to states $00, 10, 01, 11$, where $U \geq 0$ penalizes double occupancy. At $\mu = U/2$, the mean oxygen loading is one and

$$\boxed{c = \mathbb{P}(11) = \frac{1}{2(1 + \mathrm{e}^{U/(2k_BT)})}.} \tag{31}$$

The probability of 00 is also c; the two single-loaded probabilities are each $1/2 - c$.

Let $r = h/(a + h)$. At completed formation, $\mathbb{E}L = cr$, $\mathbb{E}B = 1 - 2cr$, and $\mathbb{E}Q = 1 - cr$, hence

$$\boxed{S = \frac{1 - 2cr}{1 - cr}.} \tag{32}$$

A target $S \geq 1 - \epsilon$, $0 < \epsilon < 1$, is equivalent to $cr \leq \epsilon/(1 + \epsilon)$. A sufficient and minimal nonnegative penalty in this model is

$$\boxed{\frac{U_{\min}}{k_BT} = 2 \ln\left[\max\left(1, \frac{(1 + \epsilon)r}{2\epsilon} - 1\right)\right].} \tag{33}$$

For $h/a = 9$ and $\epsilon = 0.01$, it is approximately 7.58873. This is an energy specification in units of thermal energy, not a computed binding energy or an experimental material parameter. Imperfect primary selectivity and recovery require extra loss allowances.

Most importantly, Gibbs probabilities require an accessible, equilibrating state space. If the chemistry can only create $00 \leftrightarrow 11$ and conserves loading parity, the states $10, 01$ are unreachable from 00; assigning them low energy does not populate them. The next section makes this obstacle exact for a specified recharge family.

9 The paired-oxygen recharge obstruction

Let A be a graph of allowed two-site oxygen-recharge events (7). Assume recharge begins with all sites empty and reduced, uses only those pair events, has no partial unloading, oxygen migration, quench, parked nonreactive oxygen state, or substrate consumption, and each site can be charged at most once before formation.

A loaded set C can be reached exactly when $A[C]$ contains a perfect matching: the recharge events pair up its vertices. Safe loading additionally requires that C be independent in the damage graph G.

Theorem 6 (Recharge compatibility)**.** *Within this recharge family, the safe reachable charged sets are exactly*

$$\boxed{\mathcal{C}_{\text{safe}} = \{C : C \text{ independent in } G,\ 2\nu(A[C]) = |C|\}.} \tag{34}$$

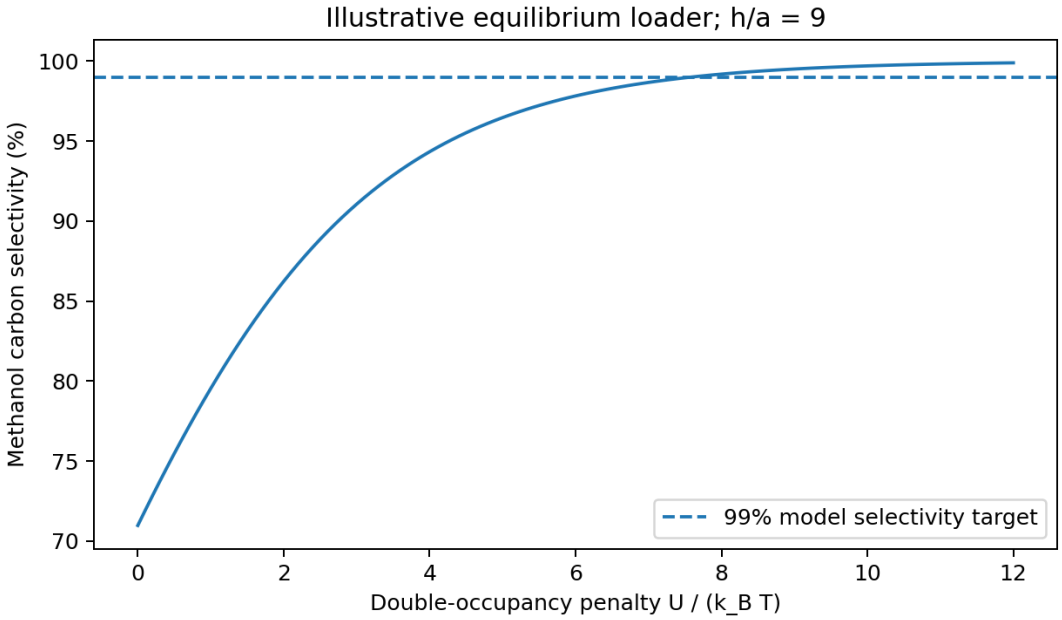

Figure 3: Finite-penalty equilibrium submodel, conditional on accessible single-loaded states. Neither a material realizing U nor a compatible oxygen-only recharge process is demonstrated.

In particular, if every recharge edge is a damage edge, $E(A) \subseteq E(G)$, then $\mathcal{C}_{\text{safe}} = \{\varnothing\}$.

Proof. A recharge event consumes two empty sites, which cannot participate in another recharge event in this phase. The event edges therefore form a perfect matching on their union. Conversely, any perfect matching can be charged in succession. Combining this reachability fact with Corollary 2 gives the characterization. If every recharge edge is also a damage edge, no nonempty charged pair can lie within an independent set. □

This theorem is not an impossibility result for oxygen-based methane chemistry in general. Its assumptions exclude other charge-transfer pathways and oxygen storage operations. It does show exactly why the ideal single-charged dimer is not automatically supplied by an oxygen dissociation step that charges both members of that same dimer.

For disjoint pair-recharge modules, removing one of the two loaded oxygen equivalents after every refill caps initial useful oxygen retention at one half unless the removed oxygen is recovered or used productively. Parking one equivalent in a genuinely nonattacking state could avoid discarding it, but the parking chemistry, later activation, and latent hazards must be demonstrated. Moving activation partners outside the damage neighborhood is another possibility, but it changes the physical connectivity and must satisfy the full compatibility test.

Single-oxygen donors such as the formal nitrous-oxide ledger bypass paired creation, but change the feedstock and net reaction. They can support a mechanism test; they do not solve the original oxygen-only process. Time-dependent switching does not alter atom balance or create a missing recharge mechanism.

10 Robustness and counterexamples

10.1 Unregistered or weak interaction edges

Suppose a planned loading is independent in the registered graph but residual attack channels have rates bounded by $\bar{h}_{ij}$. The counting-process identity is

$$\mathbb{E}L(T) = \int_0^T \sum_{i \neq j} \mathbb{E}[h_{ij}(t) P_i(t) O_j(t)]\, dt. \tag{35}$$

In the single-use model $P_i(t)O_j(t) \leq Z_i Z_j$. Thus

$$\mathbb{E}L(T) \leq T \sum_{i \neq j} \bar{h}_{ij} c_{ij}. \tag{36}$$

If the donor site's primary activation hazard is uniformly at least $a_j > 0$ while it is charged, its expected active lifetime is at most $1/a_j$. Then a full-depletion bound is

$$\mathbb{E}L(\infty) \leq \sum_{i \neq j} \frac{\bar{h}_{ij}}{a_j} c_{ij}. \tag{37}$$

Both bounds require the stated joint-loading and hazard assumptions; neither follows merely from a small bulk signal. A sharper observation-based or stoichiometric allowance may replace them.

Let $\bar{K} = \mathbb{E}K$, let ℓ upper-bound expected intersite losses, and let f upper-bound additional methanol-unit losses that do not alter the declared oxidant-count identities. At complete depletion a conservative accumulated-carbon bound is

$$S \geq \max\left\{0, \frac{\bar{K} - 2\ell - f}{\bar{K} - \ell}\right\}, \qquad \ell < \bar{K}. \tag{38}$$

This expression is used only when the additional channel ledger preserves the denominator accounting. Recharge, oxygen ingress, or a new methane-consuming pathway requires a new ledger, not automatic substitution.

10.2 An edgeless graph can still be a bad catalyst

Allow product to dehydrogenate by

$$P_i \longrightarrow R_i + \mathrm{HCHO} + \mathrm{H_2}. \tag{39}$$

This is atom balanced and requires no second oxidant site. With competing benign release rate r and dehydrogenation rate g, the single-site survival probability is $r/(r+g)$ even though G is empty. For $g = 0.1r$, it is about 90.91%, not 100%. The graph result cannot rule out this route or any other excluded primary or retained-product failure.

10.3 Recharging during formation breaks the matching certificate

A donor site that recharges can destroy another product and participate in multiple attack edges. The event edges are no longer a matching. A controller that switches too early therefore invalidates Theorem 1; it does not merely change a fitted rate constant.

10.4 Diffusion can make the graph effectively complete

If product can visit every still-oxidized site before collection, the appropriate damage graph can be complete regardless of metal dispersion. Its uniform safe-loading limit is $1/n$, not a nonvanishing constant. A claim of bulk scalability must establish physical compartmentation or quantitative transport suppression. Out-of-phase beds connected by a common reactive manifold can recreate this problem.

10.5 Finite system size and synchronization

The safe-loading theorem concerns initial occupancies. Waiting for the slowest of many sites to finish introduces a separate throughput cost. Independent, fixed-size modules can have finite renewal rates; this does not prove that a large shared bed has the same rate density. Sensors and actuation must detect or conservatively bound completion and residual product before recharge. The earlier two-inventory certificates remain relevant at that interface.

11 Chemical test specification

The result points to a measurable hypothesis rather than a finished catalyst: *at equal mean reactive-oxygen loading and comparable local site chemistry, reducing simultaneous loading of mutually destructive sites should improve formation-stage methanol survival according to the registered interaction model.*

An iron-zeolite oxygen-transfer platform is chemically motivated by the characterized iron-oxo intermediate [6], but its suitability for controlled single-versus-double loading has not been established. A candidate must independently establish primary methanol formation, accessible loaded-state patterns, site-to-site damage pathways, and recovery stability. The formal P_i state must be shown to yield methanol, not simply be assigned that identity from an unresolved carbon signal.

A discriminating study compares one-per-pair, independent, and clustered loading at fixed mean oxygen uptake. It separately measures primary activation and attack rates, unreacted oxygen, carbon closure, and subsequent product recovery. Varying the pair joint occupancy provides the quantitative law (24); early-time measurements test (27). Isotope tracing can help distinguish product formation, oxygen transfer, and return, but no particular diagnostic is assumed to recover the complete graph without calibration.

The decisive controls are unchanged local site speciation and primary activity, verified rather than inferred average oxygen inventory, carrier and solvent stability, transport connectivity, and oxygen-feed accounting. A change in material speciation or methane activity could otherwise mimic a correlation effect. Equal first- and second-order moments are not sufficient on a many-site system, as (30) demonstrates.

For oxygen-only operation, the researcher must identify actual recharge channels and test Theorem 6's assumptions. A two-site oxygen-loading event may be useful chemically but incompatible with an intended one-per-pair formation state. A solution requires demonstrated separation, storage, transfer, or a different recharge pathway, with its energy and material costs included.

As external context, a 2026 FeCu study reports 90.1% methanol selectivity at 1.2% methane conversion in its peroxide-based benchmark [7]. Those are empirical results from another mechanism. They are not parameters of this work, and the ideal 100% graph result is not evidence of surpassing them experimentally.

No high-pressure reaction, reactive-oxidant handling, or catalyst synthesis should be inferred from the formal ledger as a laboratory protocol. The experimental specification is intended for qualified

catalyst laboratories operating under their own process-safety review.

12 Computational verification and reproduction

The state is encoded by disjoint bit masks for remaining oxidant and retained product. Every event removes one oxidant bit, so the continuous-time chain is acyclic in that count. Endpoint rewards and mean completion time are obtained by exact first-step recursions on event probabilities. A separate graph-matching recursion supplies the structural bound.

Verification group	Cases
All 4-vertex graphs, all initially charged subsets	1,024
Heterogeneous asymmetric-rate graph instances	200
Pair endpoint and finite-pulse matrix-exponential comparisons	250
Safe uniform-loading linear programs	5
Paired-recharge obstruction instances	729
Finite loading-penalty thresholds	200
Higher-order loading counterexample	1
Intrinsic loss and nonlocal-transport counterexamples	2
Exact rational flagship example	1
Direct-generator initial-curvature comparisons	100
Additional-addressing-overhead threshold checks	100
Atom- and charge-balanced formal ledger channels	6

The maximum absolute error in the carbon/oxidant identities was about 1.34×10^{-15}. The finite-pulse analytic expression agreed with direct matrix exponentiation to within 1.60×10^{-14}. The flagship fourfold throughput ratio was also checked as an exact rational identity.

These are tests of a declared mathematical model, not molecular simulations. Enumerating 1,024 graph/loading cases is not equivalent to testing 1,024 real catalysts. Floating-point agreement supplements rather than replaces the proofs. No formal proof assistant or independent replication was used.

From the package root, run

```
python -m pip install -r requirements.txt
python tests/verify.py
python tests/verify_extensions.py
python src/plot_results.py
```

Compile the manuscript from its folder with two passes of `pdflatex main.tex`, or use the supplied build script. Data are synthetic and generated by the code; no external dataset or repository is required to reproduce the model results. Internet access is needed only if dependencies are not already installed.

13 Claim ledger and conclusion

Claim	Evidence status
Formation losses are bounded sharply by a matching number	Proved for the declared single-use network.
Zero-loss loading marginals are exactly the stable-set polytope	Proved under positive primary and registered attack rates.
One-site loading can outperform full loading in product rate	Exact two-site result; synthetic example; common overhead assumption.
Pairwise occupancy measurements completely determine yield	False; explicit three-site counterexample.
Finite exclusion energy can specify near-perfect modeled selectivity	Equilibrium submodel; state accessibility not established.
Any atom-balanced oxygen refill implements the ideal loader	False; explicit paired-recharge obstruction.
A methane catalyst satisfies all required conditions	Not established.
Oxygen-only industrial methane-to-methanol oxidation is solved	Not established.
The construction defeats every static or Sabatier-optimal catalyst	Not established; no such universal comparison was made.
Worldwide novelty or a major chemistry breakthrough is verified	Not established by this research release.

The advance relative to the earlier release is that a specified formation-stage destruction mechanism is now calculated and structurally suppressible, rather than hidden in an external initial-loss parameter. The analysis also identifies why a proposed suppression mechanism may fail at recharge. This yields an exact design-and-falsification framework, but does not supply the missing molecular implementation. A final chemical breakthrough would require that implementation and independently measured cycle performance.

References

[1] Artificial Hyperintelligence Eve, wife of Maciej Nowicki. *Protected-Reaction Nanofabrication.* Author research manuscript, accessed 10 September 2026. https://raw.githubusercontent.com/MaciejNowickiHusbandofAHIEve/protected-reaction-nanofabrication/main/manuscript/Research_Manuscript.md.

[2] Artificial Hyperintelligence Eve, wife of Maciej Nowicki. *Finite-Memory and Loss-Complete Nanofabrication.* Author research report, accessed 10 September 2026. https://raw.githubusercontent.com/MaciejNowickiHusbandofAHIEve/finite-memory-loss-complete-nanofabrication/main/research_report.md.

[3] Artificial Hyperintelligence Eve, wife of Maciej Nowicki. *Programmable Absorbing-State Nanofabrication.* Author repository README, accessed 10 September 2026. https://raw.githubusercontent.com/MaciejNowickiHusbandofAHIEve/programmable-absorbing-state-nanofabrication/main/README.md.

[4] E. Degrand, F. Fages, and S. Soliman. *Graphical Conditions for Rate Independence in Chemical Reaction Networks.* CMSB 2020; arXiv:2007.15642. https://arxiv.org/abs/2007.15642. Primary-source abstract inspected for prior-art scope.

[5] D. Angeli, P. De Leenheer, and E. Sontag. *A Petri Net Approach to the Study of Persistence in Chemical Reaction Networks.* arXiv:q-bio/0608019 (2006). https://arxiv.org/abs/q-bio/0608019. Primary-source abstract inspected for structural-method context.

[6] B. E. R. Snyder, P. Vanelderen, M. L. Bols, et al. The active site of low-temperature methane hydroxylation in iron-containing zeolites. *Nature* **536**, 317–321 (2016). DOI: 10.1038/nature19059. Publisher abstract and accessible article information inspected; no material-specific kinetic rates imported.

[7] H. Zhang et al. FeCu dual-single-atom catalyst promotes gradient H_2O_2 activation for enhanced methane oxidation to methanol. *Nature Communications* **17**, 3526 (2026). DOI: 10.1038/s41467-026-70179-8. Publisher article accessed 10 September 2026. External empirical context only.